Video Moment Retrieval via Natural Language Queries

Xinli Yu, Mohsen Malmir, Cynthia He, Yue Liu, Rex Wu
Amazon Alexa AI

Abstract

In this paper, we propose a novel method for video moment retrieval (VMR) that achieves state of the arts (SOTA) performance on R@1 metrics and surpassing the SOTA on the high IoU metric (R@1, IoU=0.7).

First, we propose to use a multi-head self-attention mechanism, and further a cross-attention scheme to capture video/query interaction and long-range query dependencies from video context. The attention-based methods can develop frame-to-query interaction and query-to-frame interaction at arbitrary positions and the multi-head setting ensures the sufficient understanding of complicated dependencies. Our model has a simple architecture, which enables faster training and inference while maintaining .

Second, We also propose to use multiple task training objective consists of moment segmentation task, start/end distribution prediction and start/end location regression task. We have verified that start/end prediction are noisy due to annotator disagreement and joint training with moment segmentation task can provide richer information since frames inside the target clip are also utilized as positive training examples.

Third, we propose to use an early fusion approach, which achieves better performance at the cost of inference time. However, the inference time will not be a problem for our model since our model has a simple architecture which enables efficient training and inference.

1. Introduction

Video moment retrieval (VMR) refers to the general process of associating contents across videos and text queries while maintaining the correctness of queries.

Recent surge of VMR is due to the difficulty of manual search since manual search has always been time consuming. Given a text query, VMR aims at retrieving videos segments automatically based on how well they match the text description.

Correctly identifying the most relevant time interval requires high level understanding of the video. For example, grounding the query mixing the ingredients in the video requires understanding what ingredients refer to, and being able to resolve the mixing action. Moreover, VMR requires information aggregation across temporal dimension. For example first time cat jumps up requires understanding what cat and jump refers to, in addition to grounding first by inspecting the sequence of events.

Generally, VMR models adopt two types of approaches: ranking-based approaches and discriminative approaches. Sliding window and proposal networks are two dominant approaches for moment proposal. Moment ranking is done by mapping the candidate video and the query to the same space and using a metric such as Euclidean distance. For example, [Ghosh et al., 2019] attempt to predict two probabilities at each frame, which indicate whether this frame is a starting (or ending) frame of the target video segment. [Zeng et al., 2020] propose a dense regression network to regress the temporal locations of target moment directly. **In our work, we adopt a discriminative approach since ranking-based methods are computationally expensive due to the exhaustive search in the temporal domain. Also ranking-based methods need to compute similarity between each proposal-query pair.**

Early and late fusion [Gao et al., 2017, Xu et al., 2019, Zhang et al., 2019] are two approaches to transform the candidate moment and the query to the same space. In early fusion, query information is used to map the moment video to the shared space. Late fusion transforms the moment video to the shared space without knowledge of the query, and ranks different moments using a metric distance. **In our work, we use early fusion which achieves higher accuracy at the cost of increased computations at the inference time. Due to the fact that our model has a simple architecture, the inference time will not be a problem for our model.**

One idea in current VMR approaches is the use of iterative message passing [Tan et al., 2019, Zhang et al., 2019]. The iterative procedure enriches the representation of each frame by incorporating information across all frames and query words. However, it is a computationally expensive operation that introduces additional meta parameters for the number of iterative stages. **We propose to use a multi-head attention mechanism and further a cross-attention**

mechanism, which is simple and yet verified to be effective in the experiments.

First, by utilizing the multi-head attention scheme, we derive query-enriched video features. Then by adopting a cross-attention scheme inspired by ViL-BERT [Lu et al., 2019], we derive the video-enriched query features. The query-enriched video features and video-enriched query features are concatenated together for the prediction task.

We further propose a novel moment segmentation task that helps VMR for better accuracy and performance. In particular, the moment segmentation task jointly trained with start/end prediction.

The moment segmentation task refers to the prediction of whether each time stamp belongs to the ground-truth clip or not. The start/end prediction task refers to the prediction of the probability of each time stamp being start/end.

The key contribution of the paper are two-fold:

1. We propose a moment segmentation task joint training with start/end prediction, since start/end prediction itself can be noisy due to annotators disagreement on the start and end of the video segment. Instead, by joint training the start/end prediction with moment segmentation task, this could incorporate richer information since frames inside the target clip could also be utilized as positive training examples compared to just two end points in start/end prediction.

2. We propose to use a cross-attention scheme as an early fusion approach to fuse video features with natural language query. This is a simple but efficient way compared with complicated iterative message passing based methods. Our method can achieves competitive SOTA performance on R@1 metrics, and surpassing the SOTA on high IoU metrics (R@1, IoU=0.7).

2. Related Work

VMR is a challenging task, as it not only needs to understand video content, but also requires to align the queries between video and language.

Iterative message passing is a common technique adopted in several previous VMR work. LoGAN [Tan et al., 2019] proposes an iterative graph co-attention mechanism for an early fusion of visual and language features. Moment alignment network (MAN) [Zhang et al., 2019] applies a stacked CNN to extract moment features, then use an iterative message passing to enrich the visual representation of frames.

Most of the VMR methods first learn a fused video-language embedding to generate candidate moment proposals, and then rank them according to similarity. Semantic Completion Network [Lin et al., 2020] proposes a weakly-supervised method that simultaneously learns to propose and rank solution clips based on reward function derived from query prediction task. TALL [Gao et al., 2017] performs late-fusion and embed different modalities into vectors, then measure their similarities. MLVI [Xu et al., 2019] combines segment proposal networks with encoding of the query to improve video proposals. These methods suffer from heavy computational cost and the accuracy depends on the quality of the generated candidate proposals. To address the above problem, some discriminative approaches are proposed. For example, DRN [Zeng et al., 2020] uses a regression based moment localization technique to directly regress to the target start/end position. ExCL [Ghosh et al., 2019] uses a classification based method to predict the probability of each time stamp being start/end and also a regression based method by using the expectation of the location weighted by the start/end probability distribution. In our work, we also use a discriminative approach and we propose a novel training task for multi-task learning.

Another related paper is Collaborative Experts [Liu et al., 2019], which combines a collection of pre-trained features into a single, compact video representation, which are then used to predict a similarity score to the query. We also experimented on using several video features together for richer prior information in our work.

3. Model

In this section, we will discuss our our model architecture and the variants. We propose a model that are trained end-to-end on a set of examples of annotated videos.

3.1. General Model Architecture

The Figure 1 illustrates the general architecture of the proposed method. We first use a query encoder to encode the query into embedded word features, where a bi-directional LSTM is applied and a word feature is obtained by concatenation of hidden states in both directions. Then video encoder is used to encode the untrimmed videos into video feature embeddings. In particular, we extract and use two kinds of video features encoders, i.e, the activity recognition I3D feature and the C3D features. However, any general video feature encoder could be incorporated and combined into our designed cross-attention scheme architecture.

Then, the video feature embeddings are fused with word embeddings by a cross-attention scheme to derive query-enriched video features and video-enriched query embeddings. These two embeddings are concatenated and passed into a temporal interaction module (bi-LSTM) to model the long-range temporal dependencies. Finally, a moment localization module is applied to the predict the target moment clip.

3.2. Multiple Video Encoders

Multiple video encoders and techniques are employed in our model.

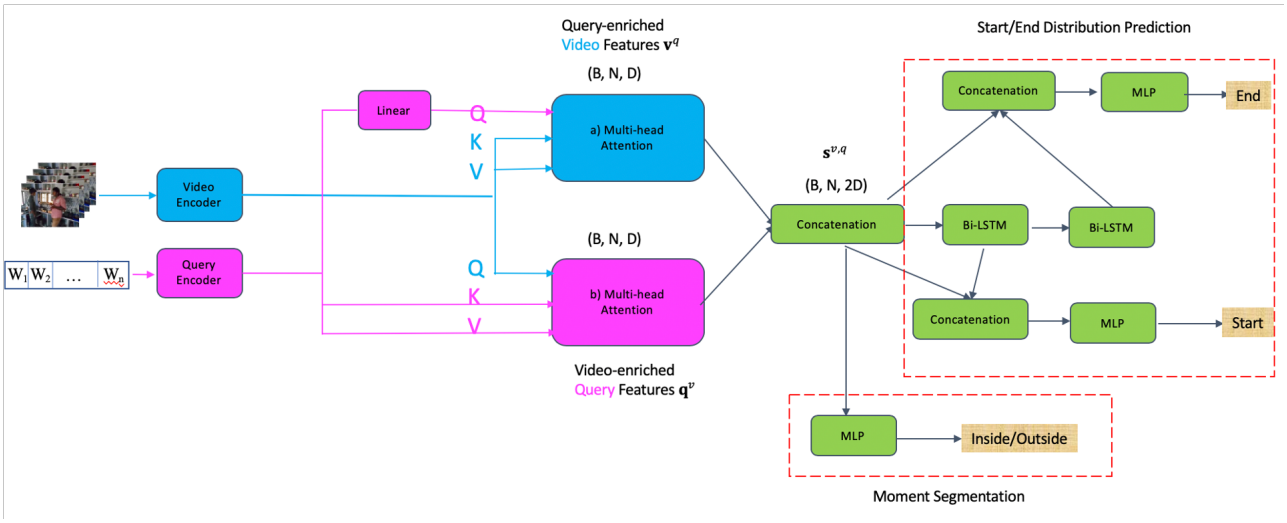

Figure 1. Overall architecture of our best performing architecture for video moment retrieval.

C3D We use C3D network [Tran et al., 2015] pre-trained on sport1M as feature encoder. The untrimmed video is divided into a sequence of 16 frames segments. A 3D CNN module is applied to extract C3D features from each 16-frame segment. The output of the 3D CNN video feature encoder module is a tensor of size $N \times D$ where $D = 500$ dimensional features and $N = T/16$ where T is the number of frames in the untrimmed video.

I3D I3D network [Carreira and Zisserman, 2017] pre-trained on Kinetics is used as feature encoder. In particular, we use a fine-tuned version for Charades-STA dataset. The videos are first pre-processed to a frame rate of 24 frames per second. The I3D network takes 64 consecutive frames as input and outputs a snippet-level feature vector.

Positional Encoding A temporal positional embedding is added to the corresponding video segment feature, and this could provide information about the relative position of each frame, thus improve accuracy. The positional encoding is formulated as a mapping from each specific position to the corresponding learned position embedding in a trainable embedding matrix as in BERT [Devlin et al., 2018].

3.3. Visual-Language Fusion

We propose to use Multi-head attention as Visual-Language fusion module. To get the desired dimension of query-enriched video embeddings, we need some transformations to be applied first on the query feature embeddings and video feature embeddings. We will describe the details of the transformation for the input features below,

Let V be the raw video input, then the video encoder embedding output

$$\mathbf{v} = f_{\text{encoder}}(V),$$

which is of size (B, N, D_v), where B is the batch size, N is the video length, D_v is the video embedding size.

Let W be the query input, then the query encoder embedding output

$$\mathbf{q} = f_{\text{encoder}}(W),$$

which is of size (B, L, D_q), where B is the batch size, L is the query length, D_q is the query embedding size.

Multi-head Attention The multi-head attention is not directly applicable to the visual-language fusion since we need a query-enriched video feature of size (B, N, D), however, applying

$$\text{MHA}(Q = \mathbf{q}, K = V = \mathbf{v})$$

outputs a query-enriched video feature of size (B, L, D), and this output is not what we desired.

To solve the above concern, we apply the following transformations on the inputs to get the our desired query-enriched video features. We use a linear layer to resize the query since the desired query-enriched video representation requires query to be the same length as video. A feedforward network is used to map the utterance to a larger space, i.e., after applying the feedforward network on $\mathbf{q}$, we get a query feature embedding $\hat{\mathbf{q}}$ of size (B, N, D).

$$\hat{\mathbf{q}} = \text{FeedForward}(\mathbf{q})$$

Further, a feedforward layer followed by RELU function is applied to the video encoder embedding outputs $\mathbf{v}$ to match the dimension with the query feature, and then positional encoding is added after to obtain the a video embedding $\hat{\mathbf{v}}$ of size (B, N, D).

$$\hat{\mathbf{v}} = \text{FeedForward}(\mathbf{v}) + \text{Positional Encoding}(\mathbf{v})$$

Thus, to get the desired query enriched video embedding, the multi-head attention we applied could be summarized as

$$\mathbf{v}^q = \text{MHA}(Q = \hat{\mathbf{q}}, K = V = \hat{\mathbf{v}})$$

Cross Multi-head Attention The output of Multi-head attention module is a single query enriched video feature embedding, i.e., attention weighted video feature embedding. However, visual enriched utterance feature embedding could also contain important information for the video moment retrieval task.

To further improve our model, we applied a cross-attention scheme to incorporate both attention-weighted video embeddings and attention weighted utterance embeddings.

In the cross-attention scheme, we use the method specified in the above section to get the attention-weighted video embeddings. More specifically, we let the Query (Q) be the transformed utterance embedding $\hat{\mathbf{q}}$ which is derived by mapping the original utterance embedding $\mathbf{q}$ to a longer length via a linear layer, and we let the Key and Value be the positional encoding augmented video embeddings $\hat{\mathbf{v}}$. Specifically, we applied

$$\mathbf{v}^q = \text{MHA}(Q = \hat{\mathbf{q}}, K = V = \hat{\mathbf{v}})$$

On the other hand, for the attention-weighted utterance embeddings in the cross-attention scheme, we use a slightly different setup compared with above section. On the contrary, we let the Query (Q) be the positional encoding augmented video embeddings $\hat{\mathbf{v}}$, and the Key (K), Value (V) be the original query embedding before the transformation to longer length. In more detail, we applied

$$\mathbf{q}^v = \text{MHA}(Q = \hat{\mathbf{v}}, K = V = \mathbf{q}).$$

Then these two embeddings are concatenated together in the embedding dimension for the following prediction task.

Thus, the fused embeddings of the two modalities $\mathbf{s}_{v,q}$ can be summarized as

$$\mathbf{s}^{v,q} = [\mathbf{v}^q, \mathbf{q}^v]$$

3.4. Multi-task Training Objectives

In the experiment section, we will test several different training tasks described below, both individually and jointly with each other to improve performance.

Moment Segmentation

The motivation for moment segmentation is that the start/end prediction is noisy due to annotators' disagreement over the annotation ground-truth boundaries, and we want to utilize more information like the inside clip frames as positive training examples. By utilizing moment segmentation as training task, we are able to select every frame within the ground truth as a positive training sample, and empirical results show that this added task is beneficial to our model performance.

In particular, for each fused embedding $\mathbf{s}_{v,q}$, at each time stamp t we apply a MLP, the MLP outputs the confidence scores for whether the time stamp t belongs to the target clip or not. After the MLP, a sigmoid function is applied over the in/out scores $S_{\text{in}}, S_{\text{out}}$ which are normalization between 0 and 1, i.e.,

$$S_{in}(t), S_{out}(t) = \text{Sigmoid}(\text{MLP}_{\text{segment}}(\mathbf{s}_t^{v,q}))$$

The loss function is binary cross entropy loss.

Start/End Location Regression Prediction

The query-enriched video embeddings $\mathbf{s}^{v,q}$ are first passed to an attentive pooling layer to get a single summarized video embedding $\mathbf{r}$, which is the weighted summation of the elements of $\mathbf{s}^{v,q}$. Then a MLP is applied over the the single summarized video embedding $\mathbf{r}$. The output is the location of the start and the end. In more details,

$$\mathbf{p} = \text{SoftMax}(\text{MLP}(\mathbf{s}^{v,q}))$$

$$\mathbf{r} = \sum_{i=1}^{T} \mathbf{p}_i \mathbf{s}_i^{v,q}$$

$$t^{\text{start}}, t^{\text{end}} = \text{MLP}_{\text{reg}}(\mathbf{r})$$

The loss function is the smooth L1 distance between the normalized ground-truth time interval and our prediction.

Start/End Distribution Prediction

First some preprocess steps are needed before being able to apply softmax to model the start/end distribution, we uniformly sample 128 time-stamps from each video if the video is longer than 128 time stamp, otherwise, we padded the shorter videos and then apply masks on these shorter videos. In particular, we first equally divide the videos longer than 128 time stamps into 128 segments then from each segment we randomly sample a single time-stamp.

1. Independent Start/End:

At each time step t, apply two MLPs on fused embedding $\mathbf{s}^{v,q}$, the output of MLP is a confidence score $S_{\text{start}}, S_{\text{end}}$ for start/end prediction. After the MLP, a softmax layer is applied to normalize the confidence scores to a distribution of being start/end.

$$S_{\text{start}}(t) = \text{MLP}_{\text{start}}(\mathbf{s}_t^{v,q})$$

$$S_{\text{end}}(t) = \text{MLP}_{\text{end}}(\mathbf{s}_t^{v,q})$$

2. Dependent Start/End:

However, in the above design, in no way the end prediction is dependent on the start prediction, thus another design where end prediction is dependent on the start prediction is proposed, i.e.,

$$\mathbf{h}_t^{P_0} = \text{LSTM}_{\text{start}}(\mathbf{s}_t^{v,q}, \mathbf{h}_{t-1}^{P_0})$$

$$\mathbf{h}_t^{P_1} = \text{LSTM}_{\text{end}}(\mathbf{h}_{t-1}^{P_0}, \mathbf{h}_{t-1}^{P_1})$$

$$S_{\text{start}}(t) = \text{MLP}_{\text{start}}(\mathbf{h}_t^{P_0})$$

$$S_{\text{end}}(t) = \text{MLP}_{\text{end}}(\mathbf{h}_t^{P_1})$$

3. Informative Dependent Start/End: Another variant is adopting the idea of ExCL [Ghosh et al., 2019] to use also the previous step prediction information and concatenate together for richer information:

$$\mathbf{h}_t^{P_0} = \text{LSTM}_{\text{start}}(\mathbf{s}_t^{v,q}, \mathbf{h}_{t-1}^{P_0})$$

$$\mathbf{h}_t^{P_1} = \text{LSTM}_{\text{end}}(\mathbf{h}_{t-1}^{P_0}, \mathbf{h}_{t-1}^{P_1})$$

$$S_{\text{start}}(t) = \text{MLP}_{\text{start}}([\mathbf{h}_t^{P_0}, \mathbf{s}_t^{v,q}])$$

$$S_{\text{end}}(t) = \text{MLP}_{\text{end}}([\mathbf{h}_t^{P_1}, \mathbf{s}_t^{v,q}])$$

Then the scores are normalized using SoftMax to give $P_{start}(t)$ and $P_{end}(t)$, i.e.,

$$P_{\text{start}}(t) = \text{SoftMax}_t(S_{\text{start}}(t))$$

$$P_{\text{end}}(t) = \text{SoftMax}_t(S_{\text{end}}(t))$$

The loss function is negative log-likelihood applied between the predicted start/end distribution and the one-hot annotated start/end label.

4. Experiments

We evaluate our model on two recent large scale datasets for the video moment retrieval task: ActivityNet Captions and Charades-STA. In this section we first introduce the datasets and our implementation details and then compare the performance of our model with other state-of-art approaches. Finally we investigate the impact of different components via a set of ablation studies and provide visualization examples.

4.1. Metrics

Following previous work, we mainly adopt "R@N, IoU=θ" as the evaluation metrics. "R@N, IoU=θ" represents the percentage of top N results that have at least one segment with higher IoU (Intersection over Union) than θ.

4.2. Datasets

ActivityNet Captions The ActivityNet Captions dataset [Caba Heilbron et al., 2015] connects videos to a series of temporally annotated sentence descriptions. Each sentence covers a unique segment of the video, describing multiple events that occur. The annotated video clips in this dataset have large variation, ranging from several seconds to over 3 minutes. On average, each of the 20K videos in ActivityNet contains 3.65 temporally localized sentences, resulting in a total of 100K sentences. We find that the number of sentences per video follows a relatively normal distribution. Furthermore, as the video duration increases, the number of sentences also increases. Each sentence has an average length of 13.48 words, which is also normally distributed.

Charades-STA Charades-STA [Sigurdsson et al., 2016] is modified by Charades. It contains 9848 videos across 157 activities. These videos were recorded by people in their own homes based on a provided script. Each video contains temporal activity annotation and sentence descriptions with start and end time to make them suitable for language-based temporal localization task.

In total, there are 13898 clip-sentence pairs in Charades-STA training set, 4233 clip-sentence pairs in test set and 1378 complex sentence queries. One query corresponds to one video clip, though each video clip could have multiple queries.

4.3. Implementation Details

We train the model in an end-to-end manner, with raw video frames and natural language query as input.

For query encoding, a bi-LSTM is adopted to encode the query embedding of 512 dimension, and we use a max query length of 25 words.

For video encoding, for C3D features the dimension is 500 and for I3D features the dimension is 1024, and we use a max video frame length of 128 frames.

In training, a batch size of 100 is used, and Adam optimization with learning rate 0.0001 is utilized.

4.4. Comparison with State-of-the-art

We compare our proposed approach on both the ActivityNet Caption and Charades-STA datasets against several prior work, for example, recent iterative message passing based methods, including LoGAN[Tan et al., 2019], MAN[Zhang et al., 2019], as well as other recent work such as DRN[Zeng et al., 2020], ExCL[Ghosh et al., 2019], SCN[Lin et al., 2020] etc.

Table 1 and **Table 2** summarize the results on ActivityNet Captions and Charades-STA datasets. Our method outperforms the all competing methods on R@1 metrics on Charades-STA dataset, and achieves better performance on the high IoU metric ("R@1,IoU=0.7") than all prior work

Method	R@1 iou=0.7
Random	3.03%
SCN [Lin et al., 2020]	9.97%
LoGAN [Tan et al., 2019]	14.54%
MLVI [Xu et al., 2019]	15.80%
ExCL [Ghosh et al., 2019]	22.40%
MAN [Zhang et al., 2019]	22.72%
DRN [Zeng et al., 2020]	31.75%
Ours	**34.41%**

Table 1. Performance Evaluation Results on Charades-STA

Method	R@1 iou=0.7
MLVI [Xu et al., 2019]	13.60%
TripNet [Hahn et al., 2019]	13.93%
ExCL [Ghosh et al., 2019]	23.9%
DRN [Zeng et al., 2020]	23.24%
Ours	**24.49%**

Table 2. Performance Evaluation Results on ActivityNet Captions

Method	R@1 iou=0.7	R@1 iou=0.5	R@1 iou=0.3
Random	3.03%	8.51%	-
LoGAN [Tan et al., 2019]	14.54%	34.68%	51.67%
MLVI [Xu et al., 2019]	15.80%	35.60%	-
ExCL [Ghosh et al., 2019]	22.40%	44.10%	-
MAN [Zhang et al., 2019]	22.72%	46.23%	-
DRN [Zeng et al., 2020]	31.75%	53.09%	-
Ours	**34.41%**	**53.23%**	**68.01%**

Table 3. Performance Evaluation Results on Charades-STA

on ActivityNet Captions dataset while getting competitive performance on other R@1 metrics.

From real-life application perspective, we are not considering R@5 based metrics. Consider Alexa customer experience, customers care more about the R@1 performance rather than R@5 performance. Customers will generally lose patience trying again when the top 1 does not work well, not to mention trying all the 5 different possibilities. For this reason, we focus on R@1 metrics rather than R@5 metrics.

4.5. Ablation Study

To evaluate the effectiveness of each component in our proposed model, we conduct ablation study on ActivityNet Captions dataset. The results are shown in **Table 3**. We observe substantial performance improvement when applying each module we proposed, especially for the metric of high IoU ("R@1,IoU=0.7").

Method	R@1 iou=0.7	R@1 iou=0.5	R@1 iou=0.3
MLVI [Xu et al., 2019]	13.60%	27.70%	45.30%
TripNet [Hahn et al., 2019]	13.93%	32.19%	45.42%
ExCL [Ghosh et al., 2019]	23.9%	41.46%	**62.21%**
DRN [Zeng et al., 2020]	23.24%	**43.78%**	-
Ours	**24.49%**	41.47%	58.59%

Table 4. Performance Evaluation Results on ActivityNet Captions

First, we perform three sets of experiments using Concatenated Transformer (CTRAN) as our fusion module, where the video and query embedding are concatenated in the length dimension, and then passed into a transformer for the visual-language fusion. The "CTRAN" fusion module is experimented with three different predictors: moment segmentation (seg), start/end regression (reg), and independent start/end distribution prediction (indep start/end). We conclude that "indep start/end" performs better than "reg", while "reg" performs better than "seg" with the fusion module "CTRAN".

Second, we perform experiments on a different fusion module Multi-Head Attention (MHA) with the three different kinds of predictors: moment segmentation (seg), start/end regression (reg), and independent start/end distribution prediction (indep start/end). We found that as in CTRAN experiments, indep start/end" consistently performs as the best predictor among the three kinds. We also conclude that compared to "CTRAN" fusion module, the "MHA" fusion module consistently works better, thus we will proceed with "MHA" as our fusion module for the follow-up experiments.

After, we further evaluate the effect of Positional Encoding (PE). In our experiments, we conclude that adding positional encoding can consistently improve the performance.

A follow-up experiment of multi-task joint training of three different tasks: moment segmentation (seg), independent start/end distribution (indep start/end) and start/end regression (reg) is conducted. From the experiment, we found start/end regression is more like a supplemental task to factor in temporal effect, helpful in joint training with independent start/end prediction which does not have mechanism of using temporal dependency. We also observe that single task "indep start/end" prediction training is noisy due to annotators disagreement of the ground-truth start/end positions, and we found that joint training with moment segmentation could help improve the performance since "seg" prediction could incorporate more in-frame information as positive examples, compared to "indep start/end" prediction with just two endpoints. We conclude that the multi-task joint training of "seg" and "indep start/end" works better in our task.

Method	**R@1 iou=0.7**	R@1 iou=0.5	R@1 iou=0.3
CTRAN+seg	11.04%	20.87%	33.26%
CTRAN+reg	12.17%	23.26%	40.28%
CTRAN+indep start/end	13.74%	25.91%	44.24%
MHA+seg	11.12%	25.42%	37.79%
MHA+reg	14.81%	28.74%	45.97%
MHA+indep start/end	16.93%	30.17%	49.27%
MHA+seg+PE	15.14%	27.57%	39.75%
MHA+reg+PE	15.43%	29.87%	48.32%
MHA+indep start/end +PE	17.26%	32.64%	51.71%
MHA+indep start/end +reg+PE	20.25%	36.78%	53.87%
MHA+indep start/end +seg+reg+PE	21.29%	37.73%	55.24%
MHA+indep start/end +seg+PE	21.86%	37.85%	55.98%
MHA+indep start/end +seg+PE	21.86%	37.85%	55.98%
MHA+dep start/end +seg+PE	22.09%	38.60%	55.96%
MHA+info dep start/end +seg+PE	22.12%	38.62%	56.27%
MHA+info dep start/end +seg+PE	22.12%	38.62%	56.27%
CMHA+info dep start/end +seg+PE	23.83%	41.78%	58.81%
CMHA+info dep start/end +seg+PE	23.83%	41.78%	58.81%
CMHA+info dep start/end +seg +PE+ connection	21.47%	40.06%	58.42%
CMHA+info dep start/end +seg+PE	23.83%	41.78%	58.81%
CMHA+info dep start/end +seg +PE+ multi-feature	23.04%	40.26%	58.51%
CMHA+info dep start/end +seg+PE	23.83%	41.78%	58.81%
multi-layer CMHA+info dep start/end +seg +PE	20.75%	37.14%	56.22%
CMHA+info dep start/end +seg+PE	23.83%	41.78%	58.81%
CMHA+info dep start/end +seg+PE+GLoVe	**24.49%**	41.71%	58.59%
CMHA+info dep start/end +seg+PE+BERT	23.17%	40.36%	57.19%

Table 5. Ablation Study on ActivityNet Captions

In the previous experiments, the end prediction is not dependent on the start prediction, while intuitively start and end predictions are possibly correlated with each other. We conducted experiments to verify the hypothesis, and two kinds of designs of start/end dependency are verified to both perform better than the case without any dependency. We also concluded that informative dependent start/end (info dep start/end) works slightly better than dependent start/end (dep start/end) and we will "info dep start/end" in the follow-up experiments.

To further improve the model, we observe that the "MHA" fusion module incorporate only the query-enriched video information, while the video-enriched query information could also be possibly helpful in the prediction tasks. Thus we did a follow-up experiment for a new design of fusion module, i.e., cross-attention (CMHA) fusion module. In particular, the "CMHA" fusion module incorporate both the query-enriched video information and the video-enriched query information, and we conclude that this design gives a performance improvement compared with single multi-head attention (MHA).

Another follow-up experiment is done for the connection algorithm of the moment segmentation prediction. Previous design the connection algorithm is very simple and we experimented a more complicated one, i.e., instead just connecting the segments with a single zero in between, we combine segments with n zeros (n being a hyper-parameter) and we filter the connected candidate segments by length and re-rank them by the number of connected zeros. We observe performance improvement in the moment segmentation outputs in IoU-1 metrics, however, the performance from moment segmentation is not surpassing our current best result. We conclude that the current design performs better.

Next, we experiment on using multiple video features to augment the model. Now the model is using a single C3D video features encoded from 3D CNN network [Tran et al., 2015], and we augment the video encoder with another video feature IDT features [Wang and Schmid, 2013]. We found that the performance is not improved with additional features, so we will proceed with a single feature.

After, an experiment with multi-layers of cross multi-head attention, i.e., "CMHA", is performed to verify if there could be a performance improvement. We conclude that stacking multi-layers of cross attention is not effective in improving the model performance.

To further improve the model, we use a GLoVe embedding initialization instead of a random initialization, and then these initialized embedding is passed in to a bi-RNN for the encoded query embeddings. We observe a performance increase in the high IoU metrics ("R@1,IoU=0.7"), while a slightly drop in the lower IoU metrics ("R@1,IoU=0.3", "R@1,IoU=0.5"). Since the high IoU metric is generally considered to be more important in the model evaluation. An improvement in high IoU metrics ("R@5, IoU= 0.5/0.7") is also observed in Charades-STA dataset. We conclude that the GloVe embedding helps improve models capability of understanding the query and increase the high IoU metric which we would care more.

5. Conclusions

In this report, we propose a cross multi-head attention based fusion model with multi-task training objectives to address the video moment retrieval task. Different from prior work, we use a cross-attention fusion approach and joint training with moment segmentation task. Our model is simpler yet more effective compared to complicated iterative message passing based methods like MAN [Zhang et al., 2019] and LoGAN [Tan et al., 2019]. Our model also achieves better or competitive performance compared with recent works like DRN [Zeng et al., 2020], ExCL [Ghosh et al., 2019], SCN [Lin et al., 2020], TALL [Gao et al., 2017] and MLVI [Xu et al., 2019] etc. The promising experimental results obtained on two widely-used datasets ActivityNet Captions and Charades-STA demonstrated effectiveness of our model.

References

[Caba Heilbron et al., 2015] Caba Heilbron, F., Escorcia, V., Ghanem, B., and Carlos Niebles, J. (2015). Activitynet: A large-scale video benchmark for human activity understanding. In *Proceedings of the ieee conference on computer vision and pattern recognition*, pages 961–970. 5

[Carreira and Zisserman, 2017] Carreira, J. and Zisserman, A. (2017). Quo vadis, action recognition? a new model and the kinetics dataset. In *proceedings of the IEEE Conference on Computer Vision and Pattern Recognition*, pages 6299–6308. 3

[Devlin et al., 2018] Devlin, J., Chang, M.-W., Lee, K., and Toutanova, K. (2018). Bert: Pre-training of deep bidirectional transformers for language understanding. *arXiv preprint arXiv:1810.04805*. 3

[Gao et al., 2017] Gao, J., Sun, C., Yang, Z., and Nevatia, R. (2017). Tall: Temporal activity localization via language query. In *Proceedings of the IEEE international conference on computer vision*, pages 5267–5275. 1, 2, 8

[Ghosh et al., 2019] Ghosh, S., Agarwal, A., Parekh, Z., and Hauptmann, A. (2019). Excl: Extractive clip localization using natural language descriptions. *arXiv preprint arXiv:1904.02755*. 1, 2, 5, 6, 8

[Hahn et al., 2019] Hahn, M., Kadav, A., Rehg, J. M., and Graf, H. P. (2019). Tripping through time: Efficient localization of activities in videos. *arXiv preprint arXiv:1904.09936*. 6

[Lin et al., 2020] Lin, Z., Zhao, Z., Zhang, Z., Wang, Q., and Liu, H. (2020). Weakly-supervised video moment retrieval via semantic completion network. *AAAI*. 2, 5, 6, 8

[Liu et al., 2019] Liu, Y., Albanie, S., Nagrani, A., and Zisserman, A. (2019). Use what you have: Video retrieval using representations from collaborative experts. *arXiv preprint arXiv:1907.13487*. 2

[Lu et al., 2019] Lu, J., Batra, D., Parikh, D., and Lee, S. (2019). Vilbert: Pretraining task-agnostic visiolinguistic representations for vision-and-language tasks. In *Advances in Neural Information Processing Systems*, pages 13–23. 2

[Sigurdsson et al., 2016] Sigurdsson, G. A., Varol, G., Wang, X., Farhadi, A., Laptev, I., and Gupta, A. (2016). Hollywood in homes: Crowdsourcing data collection for activity understanding. In *European Conference on Computer Vision*, pages 510–526. Springer. 5

[Tan et al., 2019] Tan, R., Xu, H., Saenko, K., and Plummer, B. A. (2019). wman: Weakly-supervised moment alignment network for text-based video segment retrieval. *arXiv preprint arXiv:1909.13784*. 1, 2, 5, 6, 8

[Tran et al., 2015] Tran, D., Bourdev, L., Fergus, R., Torresani, L., and Paluri, M. (2015). Learning spatiotemporal features with 3d convolutional networks. In *Proceedings of the IEEE international conference on computer vision*, pages 4489–4497. 3, 7

[Wang and Schmid, 2013] Wang, H. and Schmid, C. (2013). Action recognition with improved trajectories. In *Proceedings of the IEEE international conference on computer vision*, pages 3551–3558. 7

[Xu et al., 2019] Xu, H., He, K., Plummer, B. A., Sigal, L., Sclaroff, S., and Saenko, K. (2019). Multilevel language and vision integration for text-to-clip retrieval. In *Proceedings of the AAAI Conference on Artificial Intelligence*, volume 33, pages 9062–9069. 1, 2, 6, 8

[Zeng et al., 2020] Zeng, R., Xu, H., Huang, W., Chen, P., Tan, M., and Gan, C. (2020). Dense regression network for video grounding. In *Proceedings of the IEEE/CVF Conference on Computer Vision and Pattern Recognition*, pages 10287–10296. 1, 2, 5, 6, 8

[Zhang et al., 2019] Zhang, D., Dai, X., Wang, X., Wang, Y.-F., and Davis, L. S. (2019). Man: Moment alignment network for natural language moment retrieval via iterative graph adjustment. In *Proceedings of the IEEE Conference on Computer Vision and Pattern Recognition*, pages 1247–1257. 1, 2, 5, 6, 8